Available online at www.sciencedirect.com
SCIENCE DIRECT
Solid State Communications 138 (2006) 516–520
solid state communications
www.elsevier.com/locate/ssc

Low-temperature specific heat of double wall carbon nanotubes

B. Xiang [a], C.B. Tsai [b], C.J. Lee [c], D.P. Yu [a], Y.Y. Chen [b,*]

[a] State Key Laboratory for Mesoscopic Physics, and Electron Microscopy Laboratory, School of Physics, Peking University, Beijing 100871, People's Republic of China
[b] Institute of Physics, Academia Sinica, Taipei, Taiwan
[c] Department of Nanotechnology, Hanyang University, Seoul 133-791, South Korea

Received 9 January 2006; accepted 15 April 2006 by B.-F. Zhu
Available online 8 May 2006

Abstract

We report the analysis on the low-temperature specific heat of the double-walled carbon nanotubes (DWNTs) in the temperature range between 0.3 and 30 K, in comparison with that of the single-walled carbon nanotubes (SWNTs). The low-temperature specific heat of the SWNTs can be analyzed in terms of the acoustic phonon modes and the neighboring-tube interactions (αT^3), which are in good agreement with earlier reports. The low-temperature specific heat of the DWNTs is smaller than that of the SWNTs. Taking account of the theoretical framework of the DWNT proposed by Damnjanovic et al. and the neighboring-tube interactions (CT^3), the measured low-temperature specific heat of the DWNTs is well consistent with the theoretical predication. Our experimental results indicate that the neighboring-tube and intralayer interactions are not negligible in the low-temperature specific heat of the DWNTs.

PACS: 73.63.Fg; 74.25.Kc; 74.78.Na

Keywords: A. Carbon nanotubes; B. Low-temperature specific heat; C. Shear modulus

1. Introduction

Since the discovery in 1991, [1] the carbon nanotubes have attracted much research interests. A single-walled carbon nanotube can be thought as seamless rolling up of a graphite sheet. Due to the changes of bond angles and hybridization, deviation from the properties of the graphite is expected to be larger in smaller diameter carbon nanotubes [2]. Low-energy phonon density of carbon nanotubes is related to the mechanical properties and thermal conductivity of the carbon nanotubes. In addition, it would be helpful to study the electron–phonon scattering in carbon nanotubes [3–5]. The vibrational modes of the carbon nanotubes are studied thoroughly using Raman spectrum [6–8]. It is well known that the specific heat of the carbon nanotubes is a direct probe of the phonon energy spectrum [5]. Nopov et al. calculated the low-temperature specific heat of the isolated single-walled carbon nanotube (SWNT) and the multi-wall carbon nanotube (MWNT) [9]. Several groups reported the experimental analysis of the specific heat of the single-walled carbon nanotubes (SWNTS) [5,10–14]. Yi et al. investigated the specific heat of the multi-walled carbon nanotubes (MWNTS) [15]. However, no experimental specific heat data on DWNTS has been reported up to date.

Recently, high-purity DWNTs were produced by catalytic decomposition methods [16,17]. The DWNT is a special case of the MWNT, consisting of only two graphene sheets. Thus, the DWNTs provide an excellent opportunity to study the phonon density of the MWNTs from very small tubes [8]. Benedict et al. estimated that sufficient robust one-dimensional (1D) behavior of the heat capacity of the MWNTs at low-temperature should be observable if the tube's diameter is small enough and if the number of the layers is not too large [18]. The heat capacity for the DWNTs in the low-temperature region is predicted to be smaller than that of the SWNTs [19]. However, there is no report about the experimental results of specific heat of the DWNTs samples to our knowledge. In this paper, we will present the results of specific heat of the DWNTs samples in comparison with that of the SWNTs samples.

2. Experiment

The SWNT sample was fabricated by arc-discharge method with Y–Ni catalysts. Using micro-filtration method, more than

* Corresponding author.
E-mail address: cheny2@phys.sinica.edu.tw (Y.Y. Chen).

0038-1098/$ - see front matter © 2006 Elsevier Ltd. All rights reserved.
doi:10.1016/j.ssc.2006.04.022

90% purity of the SWNT sample was obtained. The transmission electron microscopy (TEM) image showed that most of carbon filaments were bundles of single-walled nanotubes with an average size of 30 ± 5 nm. From Raman spectrum length and diameter of the SWNTs were about 20 ± 5 μm and 1 ± 0.2 nm, respectively. The DWNTs sample was synthesized by catalytic decomposition [16,17]. Over 900% high yield of carbon nanotubes (CNTs) relative to the weight of Fe–Mo in the Fe–Mo/MgO catalyst was obtained. The low-magnified transmission electron microscopy (TEM) image in Fig. 1(a) shows the representative morphology of the bundles of the DWNTs with an average size 15–20 nm. Fig. 1(b) displays a high-resolution transmission electron microscopy (HRTEM) image, which reveals the abundance of the double-walled CNTs in the products, and it is noted that statistical HRTEM analysis revealed that more than 90% of the products were the DWNTs sample. Raman spectrum further reveals that the diameters of outer and the inner tubes of the DWNTs were in the ranges of 1.44–2.53 and 0.7–1.82 nm, respectively. The length of the sample was about 5–10 μm.

The low-temperature specific heat measurements of the SWNTs and DWNTs samples were performed down to 0.3 K using a thermal-relaxation micro-calorimeter in a ^{3}He cryostat. The SWNTs and DWNTs weighted 1.455 and 0.617 mg, respectively, were compressed into pellets with diameter

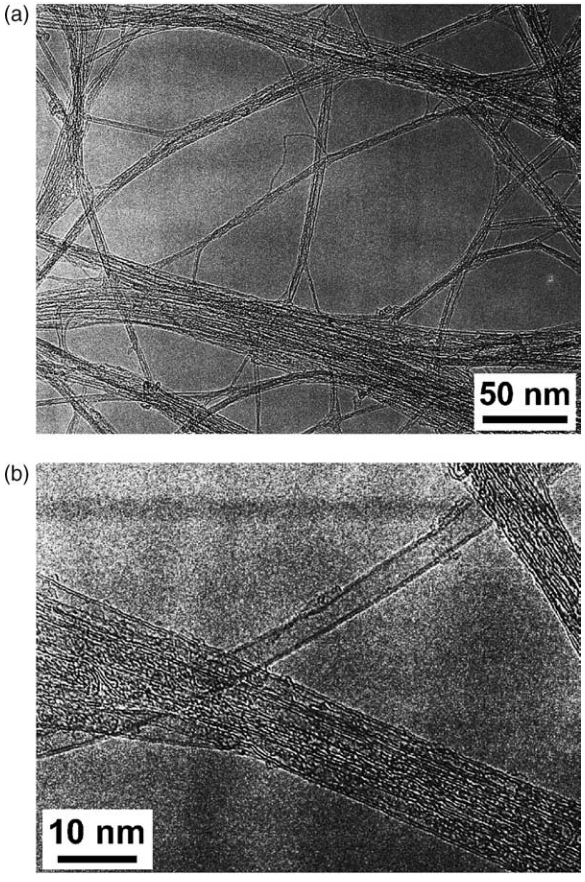

Fig. 1. (a) Low-magnified TEM image revealing the typical morphology of the bundles of DWNTs. (b) HRTEM image shows the abundance of the double-walled CNTs.

~2 mm. The pellet samples were attached into a sapphire sample holder with thermal conducting N-grease for better contact. Thin films of Ru–Al oxide and Ni–Cr alloy were deposited on the back side of the sapphire holder used as temperature sensor and joule heating element, respectively. Temperature calibration was based on a standard Cernox sensor [20]. There were four Au–Cu alloy wires between the holder and the temperature-regulated copper block for the thermal-relaxation operation and electrical connections. By taking down the time constant T of the sample temperature relaxation after each heat pulse, the specific heat can be calculated by $C=kT$, where k is the thermal conductance of the Au–Cu wires [21]. The background of the holder and the grease was properly subtracted from a separate measurement.

Carbon nanotubes have huge surface area and are known to adsorb ^{4}He gas [22]. In the ^{3}He cryostat we used, it is necessary to input the ^{4}He as exchange gas to cool the setup down to ~60 K. However, in order to get C_p of the pristine state, we first evacuated the system to 9×10^{-5} Torr at room temperature, and after cooling down to 50 K we started to pump the system and kept pumping overnight. After cooling down to 0.3 K, we reheated the sample to 30 K for 30 min, during which the temperature at the 1-K pot was kept around 1.8 K. The exchange-gas sorb attached to the 1-K pot will pump the remaining exchange gas and the desorbed gas automatically, which was released from our samples during reheating our samples.

3. Results and discussion

The phonon specific heat is defined as the temperature derivative of the energy density u

$$C_{\text{phonon}}(T)=\frac{\partial u}{\partial T}=\frac{\partial}{\partial T}\int \mathrm{d}\omega D(\omega)\frac{\hbar\omega}{\exp(\hbar\omega/kT)-1}$$

$$=k\int \mathrm{d}\omega D(\omega)\left[\frac{(\hbar\omega/kT)^2\exp(\hbar\omega/kT)}{(\exp(\hbar\omega/kT)-1)^2}\right]$$

where $D(\omega)$ is the phonon density of states. The factor in the brackets is convolved with the phonon density of states to obtain the phonon specific heat. This factor works (>0.1) for $\hbar\omega<6k_BT$, where k_B is Boltzmann's constant, while it has no contribution to the specific heat integral for $\hbar\omega>6k_BT$ [12].

The measured C_{SWNTs}/T–T^2 relationship of the SWNTs is shown in Fig. 2. For a single-wall carbon nanotube (SWNT), the specific heat can be written as $C_n=C_{\text{electron}}+C_{\text{phonon}}$. The electron contribution is much lower in the specific heat of SWNT at a relative low-temperature [9,10,13,18]. In the low-temperature range of 0.5–6 K, only the acoustic bands are activated, and the term C_{electron} can be ignored, thus the specific heat of bundles of the SWNTs can be described as $C_{\text{SWNTs}}=\alpha T^3+C_{\text{phonon}}=\alpha T^3+\beta T^x$ ($T<5.6$ K). The C_{SWNTs} is the specific heat contribution from the longitudinal acoustic mode (LA), the transverse acoustic mode (TA) and the 3D morphology of the interactions between neighboring tubes. The first term αT^3 is the specific heat contribution from the

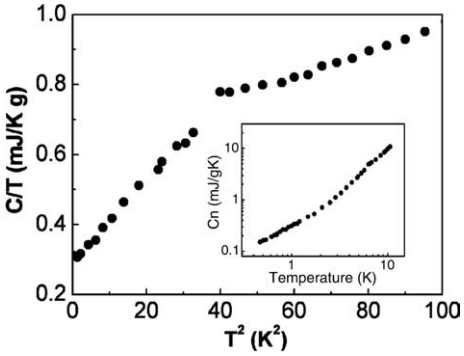

Fig. 2. The C_{SWNTs}/T–T^2 curve of the SWNTs between 0.3 and 10 K. The inset is the temperature dependence of specific heat of the SWNTs.

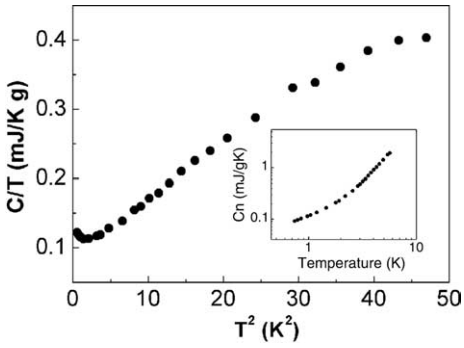

Fig. 3. The C_{DWNTs}/T–T^2 curve of the DWNTs between 0.3 and 10 K. The inset is the temperature dependence of specific heat of the DWNTs.

interaction of the neighboring nanotubes, which saturates above 5.6 K, leading to a crossover of a weaker power-law behavior in the specific heat C_{SWNTs} (the inset in Fig. 2) [5,13]. The second term βT^x is the contribution from the longitudinal acoustic mode (LA) with AT and the transverse acoustic mode (TA) with $BT^{1/2}$. If the length of the nanotube is much larger than its diameter, the x is treated as 1 [23]. From the slope and intercept of C_{SWNTs}/T–T^2 curve showed in Fig. 2, we get the value of α and β, 0.0098 and 0.2954, respectively. It is also found that the inset in Fig. 2 between 0.7 and 6 K is well fitted with the combination of power laws $0.01075T^3 + 0.3123T$, and the coefficients are very close to the value of α and β, which are directly obtained from the slope and intercept of the C_{SWNTs}/T–T^2 curve shown in Fig. 2.

Scroll up of a graphene sheet leads to splitting of the phonon band structures into 1D band structures due to the periodic boundary condition on the circumferential wave vector. The first optical sub-band edge is at $E_{sub} = 2.7$ meV [5]. At the temperature $T_{sub} \approx E_{sub}/6k_B$ ($\sim$6 K), the first sub-band begins to contribute to the specific heat of the SWNTs. It is easy to understand that the obvious behavior in the slope of C_{SWNTs}–T curve above 6 K (inset in the Fig. 2) is due to the contribution from the first optical sub-band, which is the characteristics of the quantized 1D phonon spectrum in the SWNTs.

For single-walled carbon nanotube, the acoustic phonon heat capacity can be written as $C_{ph} = 3Lk_B^2 T/\pi\hbar v \times(3.292), T << \hbar v/k_B R$, [18] where L is the tube length. Supposing that the diameter of the SWNT is about 1 nm, the specific heat of the SWNT is equal to 1.97 T calculated by dividing the heat capacity C_{ph} by the mass of a single SWNT. Thus, the specific heat of bundles of the SWNTs can be described as $C_{SWNTs} = \alpha T^3 + \beta T = C_1(mT^3) + C_2(1.97T)$, ($T < 6$ K). Here, the mT^3 term is the specific heat of the 3D phonons. As we know, $C_1 + C_2 = 1$. Thus, we calculated that m was equal to 0.0129. As a result, we obtained the $0.0129T^3$ term, which represents the specific heat from the interactions between the neighboring tubes in the bundles of the SWNTs. The diameter of the SWNTs used in our theoretic calculation conforms to the analysis of TEM and Raman spectrum.

For the DWNTs sample, the specific heat of bundles of the DWNTs can be written as $C_{DWNTs} = CT^3 + DT^x$ in the range of 0.7–6 K. The first term CT^3 is the contribution due to the interaction of neighboring nanotubes, and the second term DT^x is the contribution due to acoustic phonons. Fig. 3 shows the measured C_{DWNTs}/T–T^2 relationship of the DWNTs. The upturn at low-temperature is due to the catalysts, which can be neglected. The slope $C = 0.0067$ and intercept $D = 0.096$ in the C_{DWNTs}/T–T^2 curve can thus be obtained. Due to the large length–diameter ratio, the x is taken as 1 [23]. So the C_{DWNTs}–T curve shown in inset can be well fitted with $0.00701T^3 + 0.11009T$ between 0.7 and 5.6 K. It is obvious that the coefficients are also very close to the value of C and D, which are directly obtained from the slope and intercept of the C_{DWNTs}/T–T^2 curve in Fig. 3. It is visible that there is a crossover at 5–6 K in the inset in Fig. 3, which is due to the first optical sub-band contribution, similar to that of the SWNT sample.

It can be seen from Fig. 4 that the experimental specific heat of the DWNTs (solid circle) is smaller than that of the SWNTs (open circle). Such a difference can be explained with the intralayer interactions inside the DWNT. Damnjanovic et al. [19] reported that in the low-energy acoustic modes, the intralayer interaction in a single DWNT will cause the same type coupling of the low-energy vibrational acoustic modes, and those coupled modes can be evolved into an acoustic mode and an optical mode. Therefore, it is concluded that the intralayer interaction makes the specific heat of the DWNT significantly smaller in the low-temperature regime. In the Fig. 5, the dotted line is the theoretic specific heat of the DWNTs (5,5)@(10,10) [19] with the relation $\sim 0.17689T$,

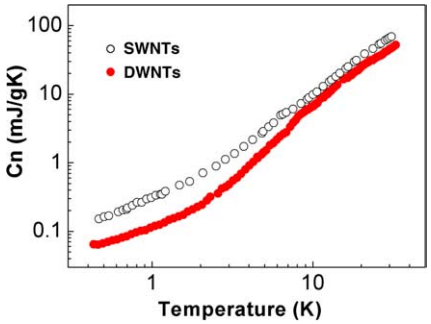

Fig. 4. The open circle curve shows the temperature of specific heat of the SWNTs. The solid circle is the temperature of specific heat of the DWNTs.

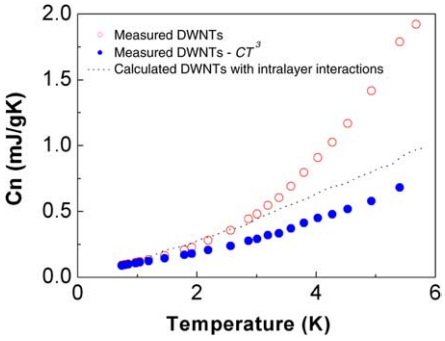

Fig. 5. The C_{DWNTs}–T curve of the DWNTs. The dotted line is the calculated data of specific heat of the DWNTs with considering the intralayer interaction [19]. The open circle is the experiment data of our DWNTs sample. The solid circle is the net specific heat in which the interaction CT^3 term was subtracted from the open circle curve (CT^3+DT^x).

which is under consideration of the intralayer interaction and without considering the interactions between neighboring tubes in the ropes. From the above discussion, the specific heat of the DWNTs sample was given by $C_{\mathrm{DWNTs}} = CT^3 + DT = C_3(nT^3) + C_4(0.17689T)$. Here, $C_3 + C_4 = 1$. Thus, we calculated that n was equal to 0.0186. Due to the larger inner diameter of our DWNTs, the actual nT^3 of our DWNTs is smaller than the calculated $0.0186T^3$ term. Compared the $0.0129T^3$ term of the SWNTs with the $0.0186T^3$ term of the DWNTs, we concluded that the specific heat of the 3D phonons in the ropes of carbon nanotubes was in the order of $10^{-2}T^3$.

As a cubic T^3 contribution to specific heat in the lower temperature range is expected from the inter-tube elastic coupling in the bundles, the C_{D} per volume can be written in according to the Debye formula [14]

$$C_{\mathrm{D}} = \alpha T^3 = \left(\frac{2\pi^2}{5}\right)\left(\frac{k_{\mathrm{B}}^4}{\hbar^3}\right)\left(\frac{T^3}{V_{\mathrm{D}}^3}\right) \tag{1}$$

where V_{D} is the mean Debye sound velocity that is defined by

$$\frac{3}{V_{\mathrm{D}}^3} = \frac{2}{V_{\mathrm{T}}^3} + \frac{1}{V_{\mathrm{L}}^3} \tag{2}$$

For bulk materials, there are two double degenerate transverse branches (V_{T}) and one longitudinal branch (V_{L}). From the mean velocity V_{D}, one can estimate the transverse velocity V_{T}, which is much smaller than the longitudinal velocity V_{L} [24]. Therefore, the Eq. (2) is approximately expressed as,

$$\frac{3}{V_{\mathrm{D}}^3} \approx \frac{2}{V_{\mathrm{T}}^3} \tag{3}$$

From the relations (1) and (3), we obtain the V_{D} value of 2.08×10^3 and 2.326×10^3 m/s for SWNT sample and DWNT sample, respectively. And $V_{\mathrm{T}} = 1.817\times10^3$ and 2.032×10^3 m/s for SWNT sample and DWNT sample. The shear modulus G can be directly deduced from V_{T}: $V_{\mathrm{T}} = \sqrt{G/\rho}$. The density ρ of SWNT sample and DWNT sample used in our calculation is about 2.32 and 2.25 g/cm^3, respectively, ($\sim$6 kbar of pressure was used to press the sample powder into a small cylindrical pellet with a diameter of $\sim$2 mm). We obtained $G = 7.2$ GPa for SWNT sample and 8.8 GPa for DWNT sample. Compared with the earlier reports, [9,14,25] the value of our SWNT bundle sample is in better agreement with the calculations for bundles of SWNTs.

4. Conclusion

In summary, we present the analysis of the specific heat of the DWNTs in comparison with that of the SWNTs. It manifests the theoretic prediction that at the relative low-temperature, the specific heat of the DWNTs is smaller than that of the SWNTs. Quantum size effects are also observed in the SWNTs and DWNTs phonon spectrum. The investigations confirm that the specific heat is a powerful technique to study the low-dimensional phonon dispersion and phonon band structures of the CNTs, in particularly for multi-walled carbon nanotubes.

Acknowledgements

Prof. Chen wants to thank the financial support from NSC 93-2112-M-001-022, Taiwan. B. Xiang is obliged to the visiting program financially and kind help during his stay in Institute of Physics, Academia Sinica, Taiwan. D.P. Yu is obliged to the financial support from the national 973 projects (No. 2002CB613505, MOST, People's Republic of China).

References

[1] S. Iijima, Nature 354 (1991) 56.
[2] R.R. Bacsa, E. Flahaut, Ch. Laurent, A. Peigney, S. Aloni, P. Puech, W.S. Bacsa, New J. Phys. 5 (2003) 1311.
[3] Z. Yao, C.L. Kane, C. Dekker, Phys. Rev. Lett. 84 (2000) 2941.
[4] C.L. Kane, et al., Europhys. Lett. 41 (1998) 68.
[5] J. Hone, B. Batlogg, Z. Benes, A.T. Johnson, J.E. Fischer, Science 289 (2000) 1730.
[6] A.M. Rao, et al., Phys. Rev. B. 275 (1997) 187.
[7] R. Saito, T. Takeya, T. Kimura, G. Dresselhaus, M.S. Dresselhaus, Phys. Rev. Lett. 57 (1998) 4145.
[8] S. Bandow, G. Chen, G.U. Sumanasekera, R. Gupta, M. Yudasaka, S. Iijima, P.C. Eklund, Phys. Rev. B. 66 (2002) 075416.
[9] V.N. Popov, Phys. Rev. B. 66 (2002) 153408.
[10] J. Hone, M.C. Llaguno, M.J. Biercuk, A.T. Johnson, B. Batlogg, Z. Benes, J.E. Fischer, Appl. Phys. A. 74 (2002) 339.
[11] J. Hone, Topics Appl. Phys. 80 (2001) 273.
[12] A. Mizel, L.X. Benedict, M.L. Cohen, S.G. Louie, A. Zettl, N.K. Budraa, W.P. Beyermann, Phys. Rev. B. 60 (1999) 3264.
[13] J.C. Lasjaunias, K. Biljakovic, Z. Benes, J.E. Fischer, P. Monceau, Phys. Rev. B. 65 (2002) 113409.
[14] J.C. Lasjaunias, K. Biljakovic, P. Monceau, J.L. Sauvajol, Nanotechnology 14 (2003) 998.
[15] W. Yi, L. Lu, D.L. Zhang, Z.W. Pan, S.S. Xie, Phys. Rev. B. 59 (1999) 9015.
[16] S.C. Lyu, B.C. Liu, S.H. Lee, C.Y. Park, H.K. Kang, C.W. Yang, C.J. Lee, J. Phys. Chem. B. 108 (2004) 2192.
[17] S.C. Lyu, B.C. Liu, C.J. Lee, H.K. Kang, C.W. Yang, C.Y. Park, Chem. Mater. 15 (2003) 3951.
[18] L.X. Benedict, S.G. Louie, M.L. Cohen, Solid State Commun. 100 (1996) 177.

[19] M. Damnjanovic, E. Dobardzic, I. Milosevic, T. Vukovic, B. Nikolic, New J. Phys. 5 (2003) 1481.
[20] Y.Y. Chen, Y.D. Yao, S.S. Hsiao, S.U. Jen, B.T. Lin, H.M. Lin, C.Y. Tung, Phys. Rev. B. 52 (1995) 9364.
[21] J.C. Ho, H.H. Hamdeh, Y.Y. Chen, S.H. Lin, Y.D. Yao, R.J. Willey, S.A. Oliver, Phys. Rev. B. 52 (1995) 10122.
[22] W. Teizer, R.B. Hallock, E. Dujardin, T.W. Ebbesen, Phys. Rev. Lett. 82 (1999) 5305.
[23] S.L. Zhang, M.G. Xia, S. Zhao, T. Xu, E. Zhang, Phys. Rev. B. 68 (2003) 075415.
[24] J.P. Lu, Phys. Rev. Lett. 79 (1997) 1297.
[25] J.P. Salvetat, et al., Phys. Rev. Lett. 82 (1999) 944.